MEaSUREs ITS_LIVE Regional Glacier and Ice Sheet Surface Velocities, Version 2

USER GUIDE

How to Cite These Data

As a condition of using these data, you must include a citation:

Gardner, A., M. Fahnestock, C. A. Greene, J. H. Kennedy, M. Liukis, L. Lopez, and T. Scambos. 2025. *MEaSUREs ITS_LIVE Regional Glacier and Ice Sheet Surface Velocities, Version 2*. [Indicate subset used]. Boulder, Colorado USA. NASA National Snow and Ice Data Center Distributed Active Archive Center. https://doi.org/10.5067/JQ6337239C96. [Date Accessed].

We also request that you acknowledge the author(s) of this data set by referencing the following peer reviewed publication:

Gardner, A. S., G. Moholdt, T. Scambos, M. Fahnstock, S. Ligtenberg, M. van den Broeke, and J. Nilsson. 2018. Increased West Antarctic and unchanged East Antarctic ice discharge over the last 7 years, *The Cryosphere*, 12(2):521–547. https://doi.org/10.5194/tc-12-521-2018.

FOR QUESTIONS ABOUT THESE DATA, CONTACT NSIDC@NSIDC.ORG

FOR CURRENT INFORMATION, VISIT https://nsidc.org/data/nsidc-0776/versions/2

National Snow and Ice Data Center

TABLE OF CONTENTS

1 DATA DESCRIPTION

This ITS_LIVE[1] data set, part of the NASA Making Earth System Data Records for Use in Research Environments (MEaSUREs) Program, consists of mean annual surface velocities (1984–2022[2]), plus climatological mean velocities (2014–2022) for 16 glacier-covered regions. The data are provided on 120 m resolution girds.

Velocities are derived by applying the autonomous Repeat Image Feature Tracking (autoRIFT) processing chain to imagery acquired by the Sentinel-1, Sentinel-2, and Landsat 4, 5, 7, 8, and 9 satellites.

1.1 Parameters

Ice velocity magnitude (v)
Ice component velocities (v_x, v_y)

1.2 File Information

1.2.1 Format

NetCDF-4 (.nc)

1.2.2 File Contents

Annual and climatological velocity files contain the parameters listed in the following tables:

Table 1. Annual Velocity File Parameter Names and Descriptions

Parameter	Description	Units	Fill/Missing Value
count	Number of image pairs used in error weighted least squares fit	count	0
floatingice	Floating ice mask. 0 = non-floating ice, 1 = floating ice	n/a	n/a
landice	Land ice mask. 0 = non-land ice, 1 = land ice	n/a	n/a
mapping	Projection details	n/a	n/a
v	Mean annual velocity determined by taking the hypotenuse of vx and vy	m/yr	-32767.0
v_error	Error weighted error for v	m/yr	32767.0

[1] Inter-Mission Time Series of Land Ice Velocity and Elevation
[2] Data scarcity and/or low radiometric quality significantly limit coverage for many regions during the earlier years of the data record. Annual coverage is nearly complete for all regions after 2013.

Parameter	Description	Units	Fill/Missing Value
vx	Mean annual velocity of sinusoidal fit to vx	m/yr	-32767.0
vx_error	Error weighted error for vx	m/yr	32767.0
vy	Mean annual velocity of sinusoidal fit to vy	m/yr	-32767.0
vy_error	Error weighted error for vy	m/yr	32767.0
x	x coordinate of projection	m	n/a
y	y coordinate of projection	m	n/a

Table 2. Climatological Velocity File Parameter Names and Descriptions

Parameter	Description	Units	Fill/Missing Value
count	Number of image pairs used for climatological means	n/a	0
dt_max	Maximum allowable time separation between image pair acquisitions included in error weighted least squares fit	days	0
dv_dt	Trend in v determined by projecting dvx_dt and dvy_dt onto the unit flow vector defined by vx and vy	m/y2	-32767.0
dvx_dt	Trend in vx determined by a weighted least squares line fit, described by an offset and slope, to mean annual vx values	m/y2	-32767.0
dvy_dt	Trend in vy determined by a weighted least squares line fit, described by an offset and slope, to mean annual vy values	m/y2	-32767.0
floatingice	Floating ice mask. 0 = non-floating ice, 1 = floating ice	n/a	n/a
landice	Land ice mask. 0 = non-land ice, 1 = land ice	n/a	n/a
mapping	Projection details	n/a	n/a
outlier_percent	Percentage of data identified as outliers and excluded from the climatological error weighted least squares fit	%	255
sensor	Sensor group (Landsat or Sentinel). 1 = L4_L5; 2 = L7; 3 = L8_L9; 4 = S1A_S1B; 5 = S2A_S2B	n/a	n/a
sensor_flag	Indicates if sensor group (see sensor variable above) is included (0) or excluded (1).	n/a	n/a
v	Velocity determined by taking the hypotenuse of vx and vy, with a time-intercept of January 1, 2018.	m/yr	-32767.0
v_amp	Climatological mean seasonal amplitude in the direction of mean flow as defined by vx and vy	m/yr	32767.0
v_amp_error	Mean seasonal amplitude error	m/yr	32767.0
v_error	Velocity error	m/yr	32767.0

Parameter	Description	Units	Fill/Missing Value
v_phase	Day of maximum climatological seasonal velocity determined from sinusoidal fit to vx and vy. Values represent numerical day of the year.	n/a	32767.0
vx	Climatological vx determined by a weighted least squares line fit (offset and slope) to mean annual vx, using a time-intercept of January 1, 2018	m/yr	-32767.0
vx_amp	Climatological mean seasonal amplitude of sinusoidal fit to vx	m/yr	32767.0
vx_amp_error	Error in vx mean seasonal amplitude	m/yr	32767.0
vx_error	Error in vx	m/yr	32767.0
vx_phase	Climatological day of seasonal maximum velocity of sinusoidal fit to vx; Values represent numerical day of the year.	n/a	32767.0
vy	Climatological vy determined by a weighted least squares line fit (offset and slope) to mean annual vy, using a time-intercept of January 1, 2018	m/yr	-32767.0
vy_amp	Climatological mean seasonal amplitude of sinusoidal fit to vy	m/yr	32767.0
vy_amp_error	Error in vy mean seasonal amplitude	m/yr	32767.0
vy_error	Error in vy	m/yr	32767.0
vy_phase	Climatological day of seasonal maximum velocity of sinusoidal fit to vy; Values represent numerical day of the year.	n/a	32767.0
x	x coordinate of projection	m	n/a
y	y coordinate of projection	m	n/a

1.2.3 File Naming Convention

Example File Names

NSIDC-0776_RGI01A_1996_V02.0.nc (annual)

NSIDC-0776_RGI01A_2014-2022_V02.0.nc (climatological)

Naming Convention

NSIDC-0776_RGI[ID]_[Year]_V02.nc (annual)

NSIDC-0776_RGI[ID]_2014-2022_V02.nc (climatological)

As shown in Figure 1, the RGI ID in file names refers to one of 16 glaciated regions as defined by the Randolph Glacier Inventory, Version 6. The spatial extent for each region is provided in Table 3 below.

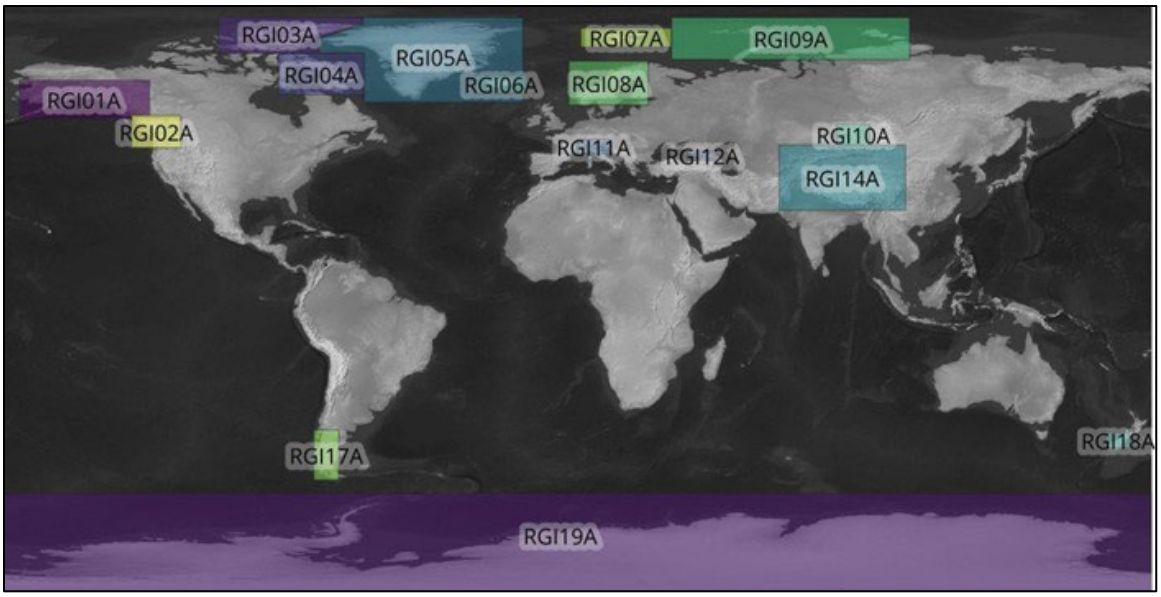

Figure 1. Approximate Locations of the 16 Randolph Glacier Inventory (RGI) Regions Used in this Data Set

1.3 Spatial Information

1.3.1 Coverage

Data are available for the 16 Randolph Glacier Inventory (RGI), Version 6 regions in Table 3. Grid min/max coordinates are specified in meters.

Table 3. Spatial Coverage by RGI Region

RGI ID	Region	EPSG	Grid x_{min}	Grid x_{max}	Grid y_{min}	Grid y_{max}
RGI01A	Alaska	3413	-3899947.5	-2700067.5	-499972.5	1999867.5
RGI02A	W. Canada/USA	32610	-40747.5	1071652.5	4995187.5	6124987.5
RGI03A	Arctic Canada (N)	3413	-1199947.5	-199987.5	-1399972.5	-600052.5
RGI04A	Arctic Canada (S)	3413	-1199947.5	-700027.5	-2899972.5	-1300132.5
RGI05A	Greenland Periphery	3413	-699907.5	899932.5	-3400012.5	-600052.5
RGI06A	Iceland	3413	900052.5	1499932.5	-2699932.5	-2200132.5
RGI07A	Svalbard/Jan Mayen	3413	900052.5	1300012.5	-799972.5	-200092.5
RGI08A	Scandinavia	3413	1900132.5	2699932.5	-2200012.5	-700132.5
RGI09A	Russian Arctic	3413	500092.5	1900012.5	-199972.5	1099867.5
RGI10A	Asia (North)	32645	300052.5	1064092.5	5094907.5	5825107.5
RGI11A	Central Europe	32632	200092.5	964132.5	4800067.5	5317267.5
RGI12A	Caucasus/Middle East	32638	6652.5	700012.5	4600027.5	4917427.5
RGI14A	High Mountain Asia	102027	-2323627.5	912412.5	-392212.5	1744387.5
RGI17A	S. Andes	32718	500092.5	1107532.5	3775027.5	5503027.5

RGI ID	Region	EPSG	Grid x_{min}	Grid x_{max}	Grid y_{min}	Grid y_{max}
RGI18A	New Zealand	32759	121012.5	700012.5	4889947.5	5399947.5
RGI19A	Antarctic/Subantarctic	3031	-2699947.5	2800012.5	-2200012.5	2399947.5

1.3.2 Resolution

120 m

1.3.3 Geolocation

Regions north of 55° N are provided in the "WGS 84 / NSIDC Sea Ice Polar Stereographic North" projection. Regions south of 56° S latitude are provided in the "WGS 84 / Antarctic Polar Stereographic" projection. High Mountain Asia data are geolocated using the "WGS 1984 Lambert for Northern Asia" projection. All other regions utilize the local Universal Transverse Mercator (UTM) projection (see Table 3).

The "mapping" variable (see "Section 1.2.2 | File Contents") contains a complete description of the coordinate reference system used for the file.

ⓘ Data files in the UTM projection specify the "grid_mapping_name" attribute in the "mapping" variable as "universal_transverse_mercator," instead of "transverse_mercator" as defined by the Climate and Forecast Metadata Conventions. As a result, some data visualization tools (e.g., Panoply Data Viewer) will plot the data correctly in the indicated UTM zone while also mirroring the data in separate, random location on the globe. Note that this only impacts how the data appear when plotted—the values in the data and grid coordinate arrays are unaffected.

1.4 Temporal Information

1.4.1 Coverage

1984–2022 (annual files, subject to data availability)
2014–2022 (climatological mean files)

1.4.2 Resolution

Annual[3]

[3] Climatological mean velocities are provided as a single file for each RGI region.

2 DATA ACQUISITION AND PROCESSING

2.1 Acquisition

This data set is generated from imagery acquired by the following satellites and sensors:

- Landsat 4, Thematic Mapper (band 2)
- Landsat 5, Thematic Mapper (band 2)
- Landsat 7, Enhanced Thematic Mapper+ (band 8)
- Landsat 8, Operational Land Imager (band 8)
- Landsat 9, Operational Land Imager (band 8)
- Sentinel-1A, Interferometric Wide mode single look complex with VV, VV+VH, HH, or HH+HV polarizations
- Sentinel-1B, Interferometric Wide mode single look complex with VV, VV+VH, HH, or HH+HV polarizations
- Sentinel-2A, Multispectral Instrument (band 8)
- Sentinel-2b, Multispectral Instrument (band 8)

Landsat images were downloaded from the USGS Registry of Open Data on AWS at https://registry.opendata.aws/usgs-landsat.

Sentinel-2 data[4] were downloaded from the European Space Agency (ESA) public Google Cloud repository at https://cloud.google.com/storage/docs/public-datasets/sentinel-2. All Sentinel-1 wide-mode data[4] were obtained from the NASA Alaska Satellite Facility Distributed Active Archive Center (ASF DAAC).

2.2 Processing Steps

Regional velocities are derived by synthesizing tens of millions of velocity estimates produced by autoRIFT, a processing chain that tracks features through time in preprocessed cross-path-row image pairs. AutoRIFT identifies matching features by using a Gaussian kernel to oversample the correlation surface by a factor of 16 and find local, normalized cross-correlation (NCC) maxima at sub-pixel resolutions.

To reduce computational demand, autoRIFT employs a downstream search that centers the NCC search template window in the search image at the downstream location of the expected displacement between the two image pairs, determined from a reference velocity. The NCC search radius is unique in both the x and y directions and varies spatially.

The processing chain uses a sparse grid, pixel-integer NCC search to determine areas of coherent correlation between image pairs, following the Normalized Displacement Coherence (NDC) filter

[4] Contains modified Copernicus Sentinel data processed by ESA

described in Gardner et al., 2018. Results from the sparse search are then used to guide a dense search, which spaces search centers such that no overlap exists between adjacent template windows. Areas of unsuccessful retrievals, as determined by the NDC filter, are searched with progressively increasing template "chip" (i.e., search areas) sizes—minimum and maximum acceptable sizes are defined geographically for each search center based on surface type (ice or rock); the spatial gradient of a reference velocity mapping; distance from the ocean; and distance from an ice edge. The data are then filtered one last time using the NDC filter, followed by a light interpolation to fill in small data gaps.

2.2.1 Image Preprocessing and Composition

Image pairs with ≤ 60% cloud cover, as indicated in the image metadata, are first aggregated into 100 km by 100 km Zarr data cubes that are optimized for time-series access.

Because geolocation errors between two images separated in time can compound, component velocities are tied to a "stable" surface—the median of each velocity component is set to zero over rock surfaces and set to a median reference velocity over slow-moving areas (< 15 m/yr).

Composite data sets are generated from the multi-sensor data cubes (one composite per data cube) as follows:

1. Add systematic errors to image pair component velocity errors based on the value of the "stable_shift_flag" on the input products[5], which tracks the velocity bias correction that was applied.
2. Use sensor-specific thresholds to discard low-quality image-pairs where excessively large v_x or v_y stable shifts have been applied.
3. Apply a filter that identifies and removes errors that occur when the feature tracking algorithm incorrectly locks onto and tracks features with similar shapes to the intended target ("skipping/locking errors").
4. Define the extent of glacierized area based on Bolch et al., 2013[6] (Greenland), Depoorter et al., 2013 (Antarctica), and the Randolph Glacier Inventory, Version 6, and a binary mask that removes all areas within 2 km of the glacier edge.
5. Exclude data with velocity magnitude > 20,000 m/yr from further analysis.
6. Apply a filter that determines the sensor-specific, maximum time separation for image pairs included in composites (provided with climatological files as "dt_max"), as skipping/locking errors increase with image-pair time separation.

Annual and climatological mean glacier velocities are then determined for each 120 m pixel using the following protocol from Greene et al., 2020:

[5] In process for public release as of this data set's publication
[6] Data set provided by F. Paul, Department of Geography, University of Zurich.

1. Apply a 15-point moving-average window filter to all input velocity data.
2. Create a matrix of coefficients with the percentage of each year spanned by each image-pair.
3. Calculate the least squares weighting for each value as 1 divided by the square of the displacement error.
4. Using the matrix from Step 2, determine annual composite outputs as the optimal fit of all valid data in an error-weighted, least-squares sense.
5. Apply the same least squares fit to determine climatological composites, but only include image-pair data with a mid date between January 1, 2014 and January 1, 2023. Mean velocity and velocity trend are determined from an error weighted linear fit to the annual data (time-intercept of January 1, 2018).

To account for artifacts specific to Sentinel-2 derived velocities:

1. All annual and climatological composites are recomputed excluding all Sentinel 2 data.
2. If the original seasonal amplitude is twice as large as the recomputed seasonal amplitude, and the difference in the seasonal amplitudes > 2 m/yr, Sentinel-2 data are excluded from the composites at that location.

If the annual velocity magnitude > 20,000 m/yr, all data for that year are excluded. Similarly, if the seasonal amplitude is > 10,000 m per year, all data for that point are excluded.

2.2.2 Mosaic Generation

Regional mosaics are created from the composites by reprojecting them into a common projection and merging the data. Overlapping composites are weighted by the maximum count of overlapping composites. Note that component velocities are rotated into the new coordinate system, such that v_x and v_y correspond to the map x and y directions.

For more information, see the MEaSUREs ITS_LIVE Regional Glacier and Ice Sheet Surface Velocities product description document.

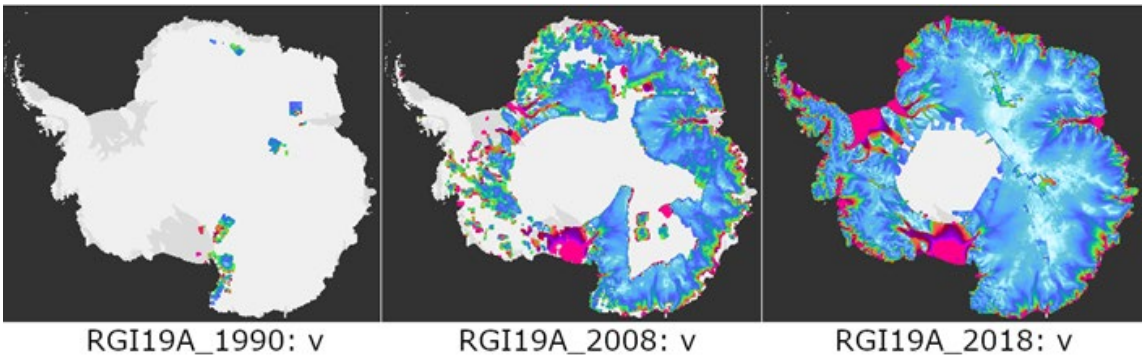

Figure 2. Sample Image Showing Annual Antarctic Ice Velocities for 1990, 2008, and 2018

2.2.3 Quality, Errors, and Limitations

Velocities are calculated in map units, which can introduce scale errors of up to a few percent depending on the projection and measurement location. Unlike Version 1, this distortion has not been corrected in Version 2. As such, the velocities in this product represent horizontal velocities that would be measured in map space. This change has the following implications:

- When using these velocities to calculate glacier flux, the flux gate cross-section no longer needs to be corrected for projection scale distortion.
- When comparing to *in situ* observations (e.g., GPS), Version 2 velocities need to be corrected for map distortion errors.

2.2.3.1 Error Computations

The uncertainty of each image pair velocity field is set equal to the standard deviation in the component velocities measured over a stable surface, after applying the geolocation offset correction (if available). If an image pair velocity field does not intersect a stable surface, the errors in v_x and v_y (parameters vx_err and vy_err) are set to the root sum of squares (RSS) of the pointing uncertainty of both images. If the image pair velocity is successfully co-registered during the creation of the annual mosaic, this error is updated to the standard deviation of the difference between the image pair component velocities and the annual mean component velocities.

This approach, while allowing for formal error propagation, typically produces errors that are unrealistically low. As such, the data producers suggest using the provided errors (vx_err, vy_err, and v_err), along with image-pair count (count), as qualitative error metrics.

3 VERSION HISTORY

Version 2 (July 2025)

4 RELATED DATA SETS

- Global Land Ice Velocity Extraction from Landsat 8 (GoLIVE), Version 1
- Landsat 8 Ice Speed of Antarctica (LISA), Version 1
- MEaSUREs Greenland Ice Velocity: Selected Glacier Site Velocity Maps from InSAR, Version 1
- MEaSUREs Annual Antarctic Ice Velocity Maps 2005-2017, Version 1

5 RELATED WEBSITES

- ITS_LIVE project
- GrIMP Data at NSIDC

- Antarctic Ice Sheet Velocity and Mapping Project (AIV)

6 REFERENCES

T. Bolch, L. Sandberg Sørensen, S. B. Simonsen, N. Mölg, H. Machguth, P. Rastner, F. Paul. 2013. Mass loss of Greenland's glaciers and ice caps 2003-2008 revealed from ICESat laser altimetry data. Geophysical Research Letters, 40(5), 875–881. https://doi.org/10.1002/grl.50270

Depoorter, M. A., J. L. Bamber, J. A. Griggs, J. T. M. Lenaerts, S. R. M. Ligtenberg, M. R. van den Broeke, and G. Moholdt. 2013. Calving fluxes and basal melt rates of Antarctic ice shelves. Nature, 502(7469), 89–92. https://doi.org/10.1038/nature12567

Gardner, A. S., G. Moholdt, T. Scambos, M. Fahnestock, S. Ligtenberg, M. van den Broeke, and J. Nilsson. 2018. Increased West Antarctic and unchanged East Antarctic ice discharge over the last 7 years. The Cryosphere, 12(2), 521–547. https://doi.org/10.5194/tc-12-521-2018

Greene, C. A., A. S. Gardner, and L. C. Andrews. 2020. Detecting seasonal ice dynamics in satellite images. The Cryosphere 14(12), 4365–4378. https://doi.org/10.5194/tc-14-4365-2020

Joughin, I., B. E. Smith, I. M. Howat, T. Scambos, and T. Moon. 2010. Greenland flow variability from ice-sheet-wide velocity mapping. Journal of Glaciology, 56(197), 415–430. https://doi.org/10.3189/002214310792447734

Lei, Y., A. Gardner, and P. Agram. 2021. Autonomous repeat image feature tracking (autoRIFT) and its application for tracking ice displacement. Remote Sensing, 13(4):749. https://doi.org/10.3390/rs13040749

Lei, Y., A. S. Gardner, and P. Agram. 2022. Processing methodology for the ITS_LIVE Sentinel-1 ice velocity products. Earth System Science Data 14(11), 5111–5137. https://doi.org/10.5194/essd-14-5111-2022

Mouginot, J., B. Scheuchl, and E. Rignot. 2012. Mapping of Ice Motion in Antarctica Using Synthetic-Aperture Radar Data. Remote Sensing, 4(9), 2753–2767. https://doi.org/10.3390/rs4092753

Rignot, E., J. Mouginot, and B. Scheuchl. 2011. Ice Flow of the Antarctic Ice Sheet. Science, 333(6048), 1427–1430. https://doi.org/10.1126/science.1208336

7 DOCUMENT INFORMATION

7.1 Publication Date

July 2025

7.2 Date Last Updated

July 2025